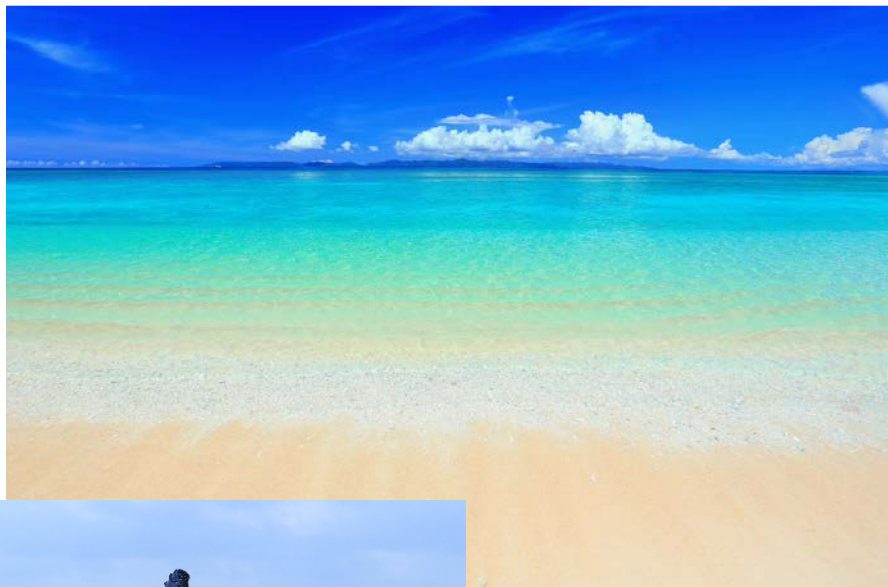


# 5<sup>th</sup> International Kyushu Colloid Colloquium

November 9, 2019

OIST Seaside House, Okinawa, Japan



## **5th International Kyushu Colloid Colloquium**

Kyushu Colloid Colloquium (KCC) was founded in 1981 by a group of leading colloid and interface scientists in Kyushu area, with an aim to promote collaboration among scientists and to encourage development and understanding in these fields. KCC has been held annually in Kyushu or western area of Japan and organized as international meetings in 2000, 2004, 2010, and 2016. In this year, the 5th International Kyushu Colloid Colloquium (IKCC) is held on November 9 in Okinawa as a post-symposium of Okinawa Colloids 2019. The purpose of this colloquium is to discuss recent progress and future prospects in colloid and interface science and technology. This colloquium will encourage interactions and to stimulate the exchange of idea among researchers in the field of assemblies of molecules and particles in solution as well as at interfaces.

### **Organizing Committee**

IKEDA, Norihiro (Fukuoka Women's Univ.)

MATSUKI, Hitoshi (Tokushima Univ.)

TAKISAWA, Noboru (Saga Univ.)

NIIDOME, Yasuro (Kagoshima Univ.)

VILLENEUVE, Masumi (Hiroshima Univ.)

MATSUBARA, Hiroki (Kyushu Univ.)

TAMAI, Nobutake (Tokushima Univ.)

GOTO, Masaki (Tokushima Univ.)

IMAI, Yosuke (Kyushu Univ.)

TAKIUE, Takanori (Kyushu Univ.)

### **Supported by**

The Division of Colloid and Surface Chemistry, the Chemical Society of Japan,

**5th International Kyushu Colloid Colloquium, 9th November 2019**  
**OIST Seaside House, Okinawa, Japan**

**Program**

**Saturday, 9th November**

Seminar Room (1F)

<b>8:30–9:05</b>	<b>Registration</b>
<b>9:05–9:15</b>	<b>Opening</b>
<b>9:15–10:00</b>	<b>KL1</b> AFM and Direct Force Measurements as Analytical Tool <b>Prof. Georg PAPASRAVROU</b> (Univ. of Bayreuth/Germany)
<b>10:00–10:45</b>	<b>KL2</b> Nanoscale Imaging of Unstained Biological Specimens in Water Using Newly Developed Scanning-electron Assisted Dielectric Microscopy <b>Prof. Toshihiko OGURA</b> (AIST/Japan)
<b>10:45–11:00</b>	<b>Coffee Break</b> (Lounge / 1F)
<b>11:00–11:25</b>	<b>IL1</b> A Challenge to Constructing Orthogonal Self-Assembly <b>Prof. Kenji ARAMAKI</b> (Yokohama National Univ./Japan)
<b>11:25–12:10</b>	<b>KL3</b> Bioinspired Design: Emergent Functional Materials from Colloidal Self-assembly <b>Prof. Nicolas VOGEL</b> (Friedrich-Alexander Univ./Germany)
<b>12:10–13:15</b>	<b>Lunch</b> (Chura Hall / 3F)
<b>13:15–13:40</b>	<b>IL2</b> Thermodynamic Study on Bilayer Phase Transitions of Twin-Tailed Cationic Surfactants <b>Prof. Masaki GOTO</b> (Tokushima Univ./Japan)
<b>13:40–14:25</b>	<b>KL4</b> Experimental Tools for Studying Lipid Organization in Complex Biomimetic Membranes <b>Prof. Frederick A. HEBERLE</b> (Univ. of Tennessee/U.S.A.)
<b>14:25–14:40</b>	<b>Coffee Break</b> (Lounge / 1F)

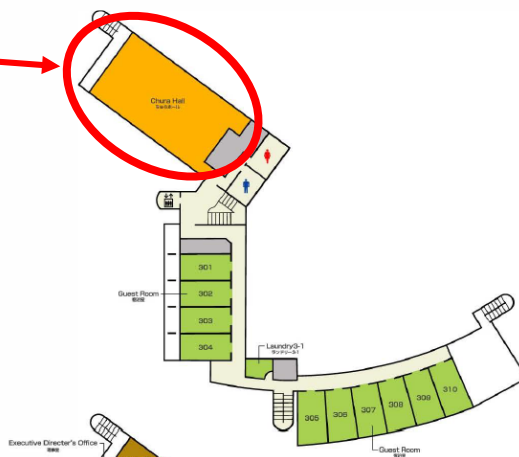
- 14:40—15:25**      **KL5**    Precipitating Surfactant into a Smart Foam Stabilizer  
**Prof. Anniina SALONEN** (University Paris Sud/France)
- 15:25—15:50**      **IL3**    Colloidal Gold Nanoparticles Used as a Mass-probe in a Living  
Body  
**Prof. Yasuro NIIDOME** (Kagoshima Univ./Japan)
- 15:50—16:50**      **Poster Session** (Lounge / 1F)
- 16:50—17:00**      **Closing**
- 17:30**                **Transportation to Naha Central (by Bus)**
- 19:30—21:30**      **Colloquium Dinner (Restaurant "Momogami")**

List of Poster

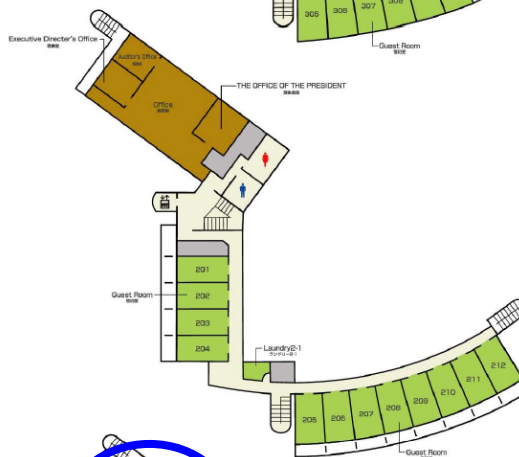
No.	Title	Authors	Affiliation
P1	Morphological and Mechanical Characterization of Synthetic ECM to Suppress Cancer Metastasis	Sona Roy, <u>Sachie Yukawa</u> , William Cortes, Ryo Kanno, Ye Zhang	Okinawa Institute of Science and Technology
P2	Supramolecular Amphiphilic Systems Based on Resorcin[4]arene: Self-Assembly and Drug-loading Capacity	<u>Ruslan Kashapov</u> , Yuliya Razuvayeva, Albina Ziganshina, Svetlana Lukashenko, Anastasiya Sapunova, and Lucia Zakharova	Russian Academy of Science
P3	Capsaicin Reorganizes Binary/Ternary Lipid Systems	<u>Neha Sharma</u> , Mun'delanji Vestergaard, Shigeru Deguchi and Masahiro Takagi	Japan Agency for Marine-Earth Science and Technology
P4	Sedimentation Particle Size and Porosity Estimation by Differential Centrifugal Sedimentation	<u>Yuichi Kato</u> , Takahiro Morimoto, Kazufumi Kobashi, Takeo Yamada, Toshiya Okazaki, and Kenji Hata	National Institute of Advanced Industrial Science and Technology
P5	Insights into the Adsorption Behavior of Surfactant onto Silica Surface with Polyelectrolytes	<u>Zilong Liu</u> , Pegah Hedayati, Ernst J. R. Sudh'oter, Robert Haaring, Abdur Rahman Shaik, and Naveen Kumar	Delft University of Technology
P6	Intentionally Added Ionic Surfactants Induce Jones-Ray Effect at Air-Water Interface	<u>Yuki Uematsu</u> , Kengo Chida, and Hiroki Matsubara	Kyushu University
P7	Aggregation Behavior in Cesium Hydroxide-Decanoic Acid Mixed Solution	<u>Taichi Koga</u> , and Masumi Villeneuve	Hiroshima University
P8	Investigation of the Adsorption of Mixed Nonionic Surfactants at the Liquid/Solid Interface by Using QCM Method	<u>Sayuri Miyamoto</u> , Tomomi Nagasaka, Kanna Hyodo, and Norihiro Ikeda	Fukuoka Women's University
P9	Particle Size Dependence of Pickering Emulsion Stability	<u>Keisuke Chiguchi</u> , Michael Gradzielski, Law Bruce, and Hiroki Matsubara	Kyushu University
P10	Effect of Alcohols and Cosmetic Oils on O/W Emulsions Stabilized by Surface Freezing Transition	<u>Hironu Sakamoto</u> , Albert Praues, Michael Gradzielski, and Hiroki Matsubara	Kyushu University
P11	Control of Line Tension and Fluid Domain Morphology by Addition of Hybrid Phospholipid in Ternary Lipid Vesicle	<u>Ryoa Kanda</u> , Yosuke Imai, and Takanori Takiue	Kyushu University
P12	Molecular Miscibility and Domain formation in Mixed Adsorbed Film of Fluoroalkanols at Alkane/Water Interface	<u>Runa Mitsuda</u> , Hajime Tanida, Toshiaki Ina, Kiyofumi Nitta, Tomoya Uruga, Yosuke Imai, and Takanori Takiue	Kyushu University
P13	Study on Effect of Hydrophilic Structure on Adsorption Behavior of Fluorinated Ester at Hexane/Water Interface	<u>Tetsuya Hotta</u> , Toshiaki Ina, Kiyofumi Nitta, Tomoya Uruga, Hajime Tanida, Yosuke Imai, and Takanori Takiue	Kyushu University
P14	Domain Formation and Molecular Miscibility in the Adsorbed Films of Mixed Fluoroalkanol-Cationic Surfactant System at Hexane/Water Interface	<u>Chikara Shirai</u> , Kosuke Saiki, Toshiaki Ina, Kiyofumi Nitta, Tomoya Uruga, Hajime Tanida, Yosuke Imai, and Takanori Takiue	Kyushu University

# DIRECTORY

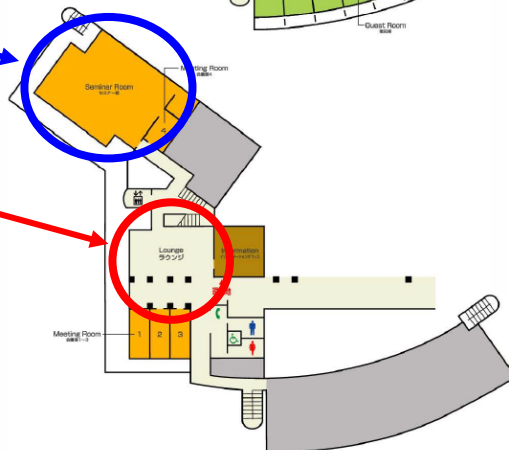
3F Chura Hall  
ちゅらホール  
Guest Room 301-310  
宿泊室 301-310



2F Office  
事務室  
Guest Room 201-212  
宿泊室 201-212



1F Seminar Room  
セミナー室  
Lounge  
ラウンジ  
Meeting Room 1-4  
会議室 1-4  
Information  
インフォメーションオフィス



 No-smoking permitted  
全館禁煙です。

**5th IKCC, 9th November 2019**

**OIST Seaside House, Okinawa**

**ORAL CONTRIBUTIONS**

KL1



## AFM and direct force measurements as analytical tool

Georg Papastavrou<sup>1,2</sup>

1 Physical Chemistry II, University of Bayreuth, Germany

2 Bavarian Polymer Institute, University of Bayreuth, Germany

Georg.Papastavrou@uni-bayreuth.de

Direct force measurements became in recent years an important analytical tool in colloid and interface science. Starting with the colloidal probe technique[1], a large number of different approaches can be followed, some will be presented here. By combining atomic force microscopy and nanofluidics it became possible to implement exchangeable colloidal probes [2] as well as to immobilize complex colloidal particles that have been previously not accessible by the colloidal probe technique.[3]

Moreover, it will be demonstrated how colloidal probes from alginate beads can be used to elucidate the adhesion of alginate to films of spider silk proteins.[4] By the combination of the colloidal probe technique and electrokinetic measurements also colloidal properties of particles from spider silk proteins can be determined.[5]

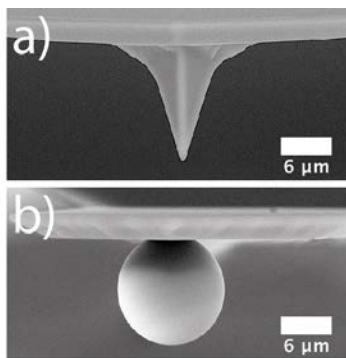


Fig. 1 (a) Standard AFM tip for imaging and (b) colloidal probe

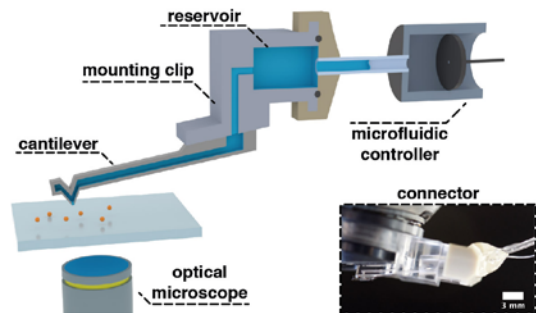


Fig. 2 Principle of the combination of AFM and nanofluidics

### References

- [1] W.A. Ducker, T.J. Senden, and R.M. Pashley, *Nature* **353** (1991) 239. H. J. Butt, *Biophys. J.* **60** (1991) 1438.
- [2] N. Helfricht, A. Mark, L. Dorwling-Carter, T. Zambelli, G. Papastavrou, *Nanoscale* **9** (2017) 9491.
- [3] A. Mark, N. Helfricht, A. Rauh, M. Karg, G. Papastavrou, *G. Small* (2019), doi:10.1002/sml.201902976.
- [4] N. Helfricht, E. Doblhofer, V. Bieber, P. Lommes, V. Sieber, T. Scheibel, G. Papastavrou, *Soft Matter* **13** (2017) 578.
- [5] N. Helfricht, M. Klug, A. Mark, V. Kuznetsov, C. Blüm, T. Scheibel, G. Papastavrou, *Biomaterials Science* **1** (2013) 1166. N. Helfricht, E. Doblhofer, J.F.L. Duval, T. Scheibel, G. Papastavrou, *J. Phys. Chem. C* **120** (2016) 18015.

## Nanoscale imaging of unstained biological specimens in water using newly developed scanning-electron assisted dielectric microscopy

Toshihiko Ogura, and Tomoko Okada

Biomedical Research Institute, National Institute of Advanced Industrial Science and Technology (AIST), Tsukuba, Japan  
t-ogura@aist.go.jp

Scanning electron microscopy (SEM) has been widely used to nanoscale observation of various biological specimens. However, usual SEM observations of the specimens under high vacuum conditions require specific sample preparation including negative staining, cryo-techniques and metal coating to avoid electrical radiation damage. Wet biological specimens have been examined using atmospheric holders, but they suffer heavy radiation damage caused by electron beam (EB).

We recently developed a new nanoscale imaging technology named a scanning-electron assisted dielectric-microscopy (SE-ADM) based on SEM [1-2]. Our system provides high-contrast imaging of the unstained and unlabeled biological specimens in water using an atmospheric sample holder comprising two 50-nm-thick silicon nitride (SiN) films (Fig. 1a). The upper SiN film, which is coated with 15-nm-thick tungsten (W) layer, is irradiated using a focused scanning EB. Irradiated electrons are scattered and absorbed in the W layer causing a negative electric-field potential at the irradiated position. This negative potential transmitted to the bottom SiN film through the biological specimens in water (Fig. 1b) [1]. In this method, the biological samples are not directly irradiated by the EB and can be escaped from electron radiation damage [1].

The intact bacteria (*Rhodobacter capsulatus*) immersed in water in the sample holder were observed using the high-resolution SE-ADM system at 10,000 $\times$  magnification, 3.6-kV EB acceleration [2]. The intact bacteria were visible with clear white contrast; the inner structure exhibited complex undulation (Fig. 2a). We also used SE-ADM to analyze whole milk specimen in an intact liquid condition [3]. The whole milk mainly comprises milk-fat globules and casein micelles. The dielectric image of untreated whole-milk shows milk-fat globules of large white spheres and casein-micelles of small black particles (Fig. 2b). Further, our system clearly visualized unstained and unfixed cancer cells in medium (Fig. 3) [4]. Figure 3a clearly shows intracellular structures, for example nucleus and endoplasmic reticulum (ER). The SE-ADM images show various vesicles and/or ER near the nucleus (Fig. 3b). Two enlarged vesicles of red-boxed area in Fig. 3b clearly reveal a spherical shape with rough surface membrane (Fig. 3c, d). The vesicles were found to be interconnected [4]. Finally, we directly observed the adhesion molecules on the cells [5, 6] and the living osteoblasts under mineralizing conditions [7].

In summary, we developed a SE-ADM system based on SEM which enables high-resolution imaging of various intact biological specimens in water without radiation damage. Our system can be applied to diverse liquid samples across broad range of scientific fields, for example, nanoparticle, nanotube and organic materials.

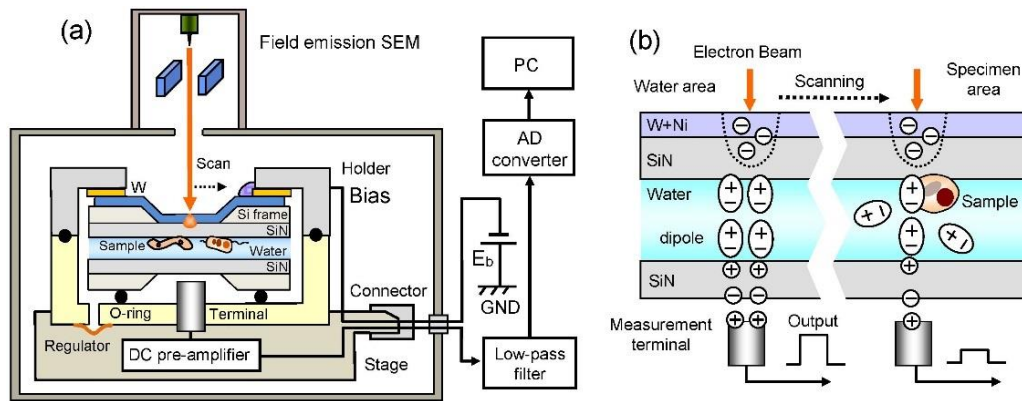


**Figure 1.** Experimental set-up of SE-ADM system. (a) Schematic of the SE-ADM system based on field emission SEM. (b) Schematic of our hypothesis of the SE-ADM imaging method. (Ref. [1])

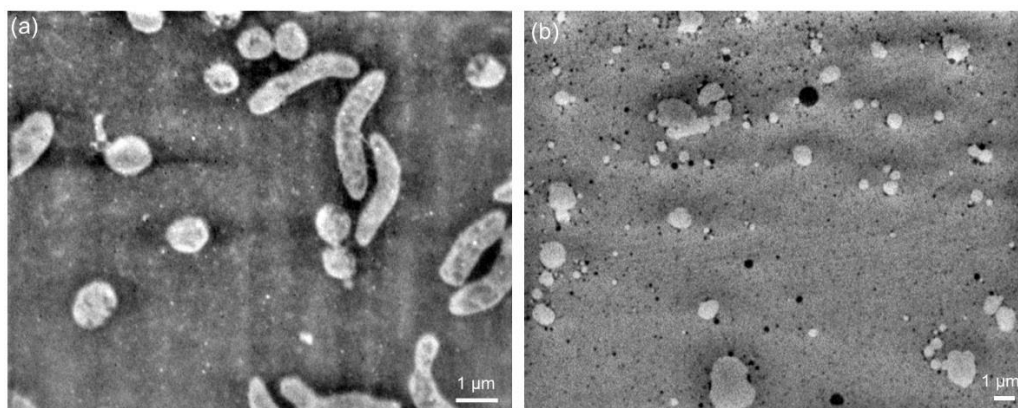


**Figure 2.** Imaging of intact bacteria and whole milk using SE-ADM system. (a) The reversed contrast image of bacteria. (Ref. [2]) (b) The dielectric image of untreated whole-milk using SE-ADM system. (Ref. [3])

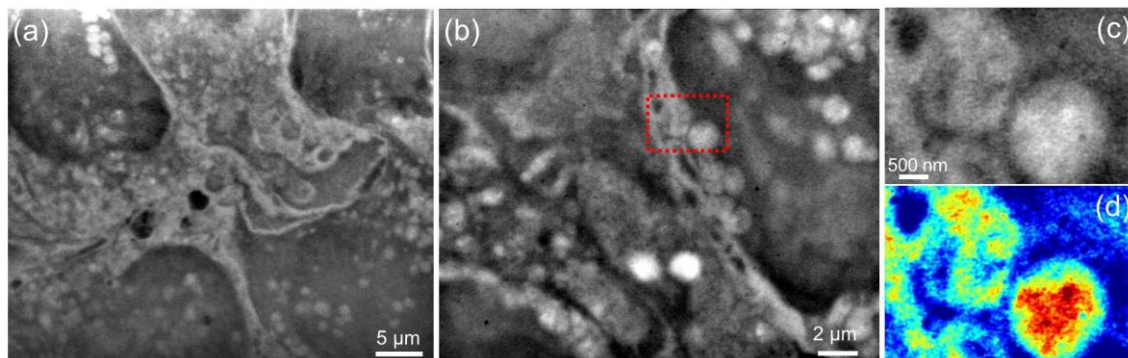


**Figure 3.** Observation of intact cells in medium using SE-ADM (a) Dielectric image near the nucleus region. (b) Dielectric image of another vesicle-rich region. (c) Enlarged images of the vesicle regions indicated in the red boxes in (b). (d) Pseudo-colour map of (c). (Ref. [4])

## References

- [1] T. Ogura, PLOS ONE **9** (2014) e92780. [2] T. Ogura, Biochem. Biophys. Res. Commun. **459** (2015) 521-528. [3] T. Ogura and T. Okada, Biochem. Biophys. Res. Commun. **491** (2017) 1021-1025. [4] T. Okada and T. Ogura, Sci. Rep. **6** (2016) 29169. [5] T. Okada and T. Ogura, Sci. Rep. **7** (2017) 43025. [6] T. Okada and T. Ogura, PLOS ONE **13** (2018) e0204133. [7] T. Iwayama, T. Okada *et al.*, Sci. Adv. **5** (2019) eaax0672.

**Acknowledgements:** We thank Ms. Yoko Ezaki and Miho Iida for their technical assistances. This study was supported by JSPS KAKENHI Grant-in-Aid for Scientific Research (B) (15H04365, 19H03230).

KL3

**Bioinspired design: Emergent functional materials from colloidal self-assembly**

Nicolas Vogel

Institute of Particle Technology, Friedrich-Alexander University Erlangen-Nürnberg

e-mail: nicolas.vogel@fau.de

The spontaneous organization of individual building blocks into ordered structures is extensively used in nature and found at all length scales, from crystallization processes, via composite materials, to living cells constituting complex tissue. Understanding the relationship between building blocks, environmental conditions, and resulting structure is of fundamental importance for controlling materials properties.

An interesting class of building blocks are colloidal particles, which can be synthesized with high precision in the nanometer range. Under the right conditions, these particles can self-assemble into ordered structures in two- and three dimensions, providing a simple access to nanostructured materials.

In my lecture, I will introduce simple processes to control the self-assembly process of such colloidal particles and highlight how such self-assembled structures can be used to mimic functional properties arising in the natural world. I will highlight two aspects of such bioinspired materials. First, defined surface structures are responsible for the highly repellent surfaces of the Lotus and the Pitcher plant, which obtain self-cleaning properties by controlling the contact with a contaminating medium. Controlled surface features in man-made materials can mimic these repellent properties and allow for the design of coatings that are not stained by a range of different liquids and fluids. Second, the beautiful colors observed in the natural world often arise from defined nanoscale structures within the biological materials, which can be ideally replicated by colloidal self-assembly, allowing for the design of materials with fascinating optical properties.

KL4

## **Experimental tools for studying lipid organization in complex biomimetic membranes**

*Frederick A. Heberle*

The three-dimensional architecture of biological membranes has functional consequences for living cells. In the outer leaflet of the plasma membrane, lipids are thought to organize into nanoscopic ordered fluid domains, with diverse evidence supporting participation of these “rafts” in membrane processes including protein sorting and signaling. Cells also actively maintain an asymmetric distribution of different lipid types between the plasma membrane’s inner and outer leaflets that can alter the structure and properties of the bilayer. In this talk, I will describe experimental techniques capable of characterizing nanostructural details of complex biomimetic membranes, including Förster resonance energy transfer, small-angle neutron and X-ray scattering, and cryogenic electron microscopy.

Li Zhang<sup>1,2</sup>, Alesya Mikhailovskaya<sup>1</sup>, Anniina Salonen<sup>1</sup>

1 Laboratoire de Physique des Solides, Université Paris Sud, France

2 School of Materials Science and Engineering, Xi'an University of Science and Technology, China

anniina.salonen@u-psud.fr

Foams are used in food products, for cleaning purposes, to extract petrol and in many other industrial processes and products. This makes the control of their properties and stability such important questions. Aqueous foams are collections of gas bubbles in water and they are intrinsically unstable, which means that they will always eventually disappear. The lifetime of the foams depends on the efficiency of the used stabilisers in slowing down the different mechanisms of ageing.

We are most familiar with surfactant-stabilised foams. In general such foams are rather unstable and disappear within hours. However, we have shown that the presence of salt can change foam stability dramatically. The addition of salt can lead to the precipitation of surfactant, where the surfactant crystals can behave as particles at interfaces (as seen in the photograph). The stability of these foams depends on the properties of the precipitate, which in turn can be controlled by both the concentration, and the type of salt used. Therefore we can create rather versatile superstable foams, which destabilize upon command, making simple surfactant foams surprisingly smart.

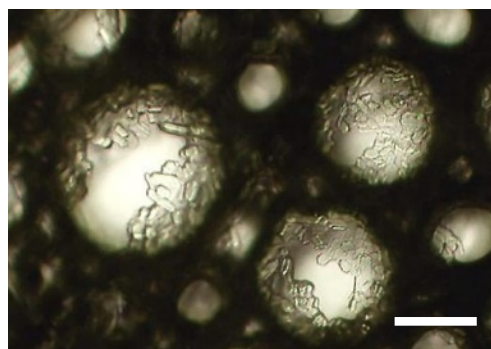


Fig. 1 Photo of surfactant-crystal stabilised bubbles (scale bar 200 $\mu$ m)

#### References

- [1] L. Zhang, A. Mikhailovskaya, P. Yazhgur, F. Muller, F. Cousin, D. Langevin, N. Wang, and A. Salonen, *Angewandte Chemie Int. Ed.* **54** (2015) 1
- [2] L. Zhang, L. Tian, H. Du, S. Rouzière, N. Wang, and A. Salonen, *Langmuir* **33** (2017) 7305

Kenji Aramaki

Graduate School of Environment and Information Sciences, Yokohama National University, Japan

aramaki-kenji-cr@ynu.ac.jp

## **1. Introduction**

There are a number of bulk systems consisting of different self-assembled structures without interfering each other. The cell which is one of such typical examples exhibits excellent functionality and morphological stability by supporting a soft lipid bilayer membrane with a fibrous protein complex called a cytoskeleton. An important point in cell structure is that each self-assembled structure plays a different role, and that both self-assembled structures are essential for cell functions. This means that the two structures complement each other but do not affect each other. A state in which things, concepts, systems, etc. coexist independently of each other is called “orthogonality”. In the science of molecular assembly, surfactants, lipids, supramolecules, etc. are often treated as independent research objects. However if one learns from the cell structure, construction of orthogonal systems that combines different molecular assemblies is necessary to reach a further height in the science of molecular assembly. It should also impart highly functionalized soft matters that can be useful for various applications. From this point of view, research has been conducted on orthogonal self-assembled systems in which a surfactant / lipid assembly and self-assembled fibrillar networks (SAFiNs) of low molecular weight gelators (LMGs) coexist. [1-3] In these studies, low-molecular weight hydrogelators are used for gelation in aqueous solution-based surfactant systems. It seems natural idea at first glance, but in recent years, when we started a similar study in our laboratory, we discovered that aqueous micellar and lamellar liquid crystalline phases can be gelled by using a low-molecular weight organogelator, which we termed surfactant mediated gelation (SMG). Normally, an organogelator is insoluble in water and therefore cannot form hydrogel. However, as shown in Fig. 1, the surfactant assemblies solubilize organogelator in water, followed by fiber formation. By this way we can do “hydrogelation by organogelator”. In this presentation, the preparation, structures and mechanical properties of the orthogonal self-assembled systems in which surfactant micelles, wormlike micelles or lamellar liquid crystals coexist the SAFiNs of organogelator will be presented.

## **2. Gelling Micellar Solution by SMG [4]**

Organogelator, 12-hydroxyoctadecanoic acid (12-HOA), which gels various organic solvents but not water. However, it is possible dissolving 12-HOA in an aqueous surfactant micellar solution. A clear transparent solution was obtained when 12-HOA was solubilized in an aqueous micellar solution of cationic surfactants such as cetyltrimethylammonium bromide (CTAB) at 80°C. Then the sample was gradually cooled to a room temperature and a gel (Fig.1) was obtained. Minimum gelation concentration and viscoelasticity was influenced by the hydrophobic chain length and surfactant molecular structure as well as the micellar shape. The dynamic viscoelasticity measurement results

show a gel or elastic behavior. The gelled wormlike micellar phase exhibits higher viscoelasticity than the gelled micellar phase. However, compared to an organogel obtained with 12-HOA and n-decane, hydrogels have lower viscoelasticity, suggesting some of 12-HOA molecules remain in surfactant micelles after the SMG process and remain solubilized in micelles. TEM photos (Fig.1) of dried sample of the hydrogels obtained by SMG shows the formation of a fibrous aggregate similar to that formed in organogels by 12-HOA [5, 6]. In order to confirm the presence of micelles in the hydrogel UV-vis and small angle scattering were performed. From the above study, it was found that the hydrogels (gelled micellar/wormlike micellar phase) obtained by SMG is orthogonal molecular assembled systems.

### 3. Gelling Lamellar Phase by SMG [7]

12-HOA was also added to lamellar liquid crystal formed by didodecyldimethylammonium bromide (DDAB) and the same treatment was carried out to obtain a gel. Dynamic viscoelasticity measurements showed that the gelled samples have a higher storage modulus ( $G'$ ) and loss modulus ( $G''$ ) than the non-gelled samples, indicating that SAFiNs of 12-HOA improve the mechanical properties. TEM and SWAXS measurements on the gels revealed the coexistence of the surfactant lamellar phase and 12-HOA gel fibers.

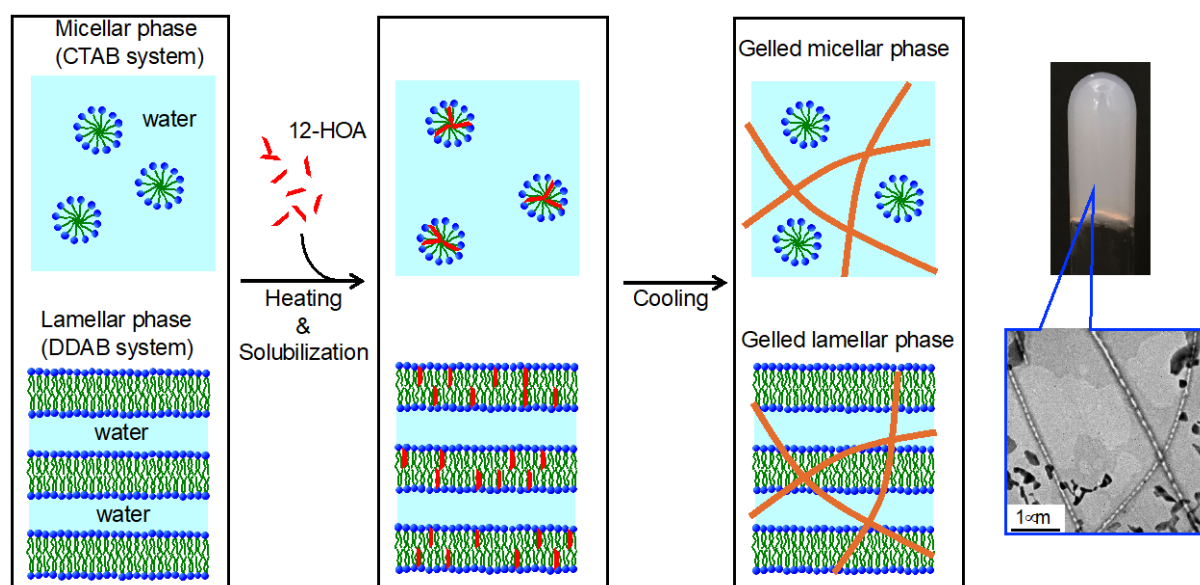


Figure 1 – Preparation of hydrogels through “Surfactant Mediated Gelation (SMG)”

### References

- [1] A. Brizard, M. Stuart, K. van Bommel, A. Friggeri, M. de Jong and J. van Esch, *Angew. Chem. Int. Ed.* **47** (2008) 2063.
- [2] J. Boekhoven, A. M. Brizarda, M. C. A. Stuartb, L. Florussea, G. Raffyc. A. Del Guerzoc and J. H. van Esch, *Chem. Sci.* **7** (2016) 6021.
- [3] C. Stubenrauch and F. Gießelmann, *Angew. Chem. Int. Ed.* **55** (2016) 3268.
- [4] K. Aramaki, S. Koitani, E. Takimoto, M. Kondo and C. Stubenrauch, accepted.
- [5] T. Tachibana and H. Kambara, *Bull. Chem. Soc. Jpn.* **42** (1969) 3422.
- [6] M. Laupheimer, N. Preisig, C. Stubenrauch, *Colloids Surf. A*, **469** (2015) 315.
- [7] S. Koitani, S. Dieterich, N. Preisig, K. Aramaki and C. Stubenrauch, *Langmuir* **33** (2017) 12171.

## Thermodynamic Study on Bilayer Phase Transitions of Twin-Tailed Cationic Surfactants

Masaki Goto<sup>1</sup>, Anna Tanaka<sup>2</sup>, Makiko Motohashi<sup>2</sup>, Nobutake Tamai<sup>1</sup>, and Hitoshi Matsuki<sup>1</sup>

<sup>1</sup> Grad. Sch. of Tech. Indus. & Soc. Sci., Tokushima University, Japan

<sup>2</sup> Grad. Sch. of Adv. Tech. & Sci. Tokushima University, Japan

goto@tokushima-u.ac.jp

Cationic surfactants with double alkyl chains like dialkyldimethylammonium halides ( $2C_nXs$ ) form vesicle bilayers in aqueous solutions. The bilayer properties of one of representative  $2C_nXs$ , diocatadecyldimethylammonium bromide ( $2C_{18}Br$ ), have been studied in detail by various experimental techniques. However, there have been few studies with respect to the effect of hydrophobic alkyl-chain length or hydrophilic counter ions on physico-chemical properties of the  $2C_nX$  bilayers. In our previous study, we have examined phase transitions of the  $2C_nBr$  ( $n = 12, 14, 16, 18$ ) bilayers under atmospheric and high pressure<sup>1</sup>. From the temperature ( $T$ )-pressure ( $p$ ) phase diagrams constructed and the thermodynamic quantities of the phase transitions obtained for the  $2C_nBr$  bilayers, it turned out that the hydrated crystal ( $L_c$  or  $L_{c(1)}$ ) phase is stable in all  $2C_nBr$  bilayers but the gel ( $L_\beta$ ) phase is fundamentally metastable in all bilayer except for the high-pressure region of the  $2C_{18}Br$  bilayer, and that phase behavior becomes so complicated with the chain elongation.

Recently, we investigated the effect of alkyl-chain length on the phase behavior and thermodynamic quantities of phase transitions for dialkyldimethylammonium chloride ( $2C_nCl$ ) bilayers by means of differential scanning calorimetry (DSC) under atmospheric pressure and light-transmittance measurements under high pressure. The phase transition-temperatures and -enthalpies ( $\Delta H$ ) of the  $2C_nCl$  bilayers increased with an increase in chain length. Unlike the case of the  $2C_nBr$  bilayers, the stability of the  $L_\beta$  phase of the  $2C_nCl$  bilayers changed depending on the chain length: the  $L_\beta$  phases of the bilayers of  $2C_nCl$  with medium alkyl chains are stable while those with long alkyl chains are metastable (Fig. 1). Comparing the transition-temperatures and  $\Delta H$  values of the  $2C_nCl$  bilayer with those of  $2C_nBr$  ones, the present result revealed that the rule of lyotropic series, namely Hoffmeister series of counter ions is applicable to the  $2C_nX$  bilayers.

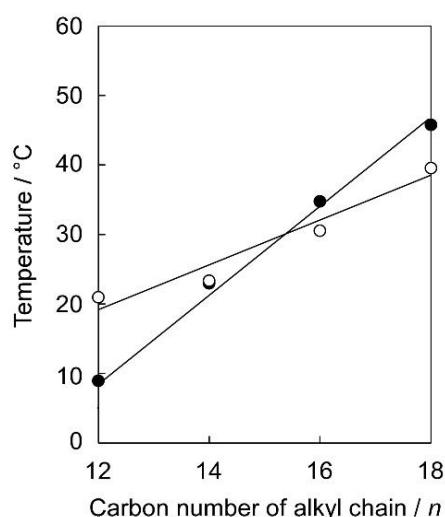


Fig. 1. Phase-transition temperatures of the  $2C_nCl$  bilayers at 0.1 MPa: (○)  $L_\beta/L_\alpha$  transition, (●)  $L_c$  (or  $L_{c(1)})/L_\beta$  or  $L_c$  (or  $L_{c(1)})/L_\alpha$  transition.

### References

- [1] M. Goto, S. Ishida, Y. Ito, N. Tamai, H. Matsuki, and S. Kaneshina, *Langmuir* **27**, (2011) 5824.

Yasuro Niidome

Faculty of Science and Engineering, Kagoshima University, Japan

yniidome@sci.kagoshima-u.ac.jp

Mass-probe produces specific ions under pulsed-laser irradiation. These specific ions can act as probe-ions for the target molecules. Gold nanoparticles generate gold ions under pulsed-laser irradiation. In the absence of matrix molecules, organic molecules were rarely desorbed, and gold ions were preferentially obtained. The gold ions were advantageous in determining the distribution of gold nanoparticles in tissue sections<sup>1-3</sup> and on blotting membranes.<sup>4-6</sup> It was shown that the gold nanoparticles acted as a sensitive mass probe. The distribution and the dispersion of the nanoparticles were, however, not homogeneous on the membrane.

To make homogeneous dispersion, gold nanoparticles were dispersed in a gelatin solution and made gelatin sections using a cryomicrotome. Gold ion intensities from the gelatin sections were expected to be reproducible. Here, we evaluated LDI efficiencies of star-shaped gold nanoparticles (nanostars) as well as spherical gold nanoparticles (nanospheres). Keeping their absorbance as  $0.043 \text{ /cm}^{-1}$  at 355 nm. All the gelatin sections (thickness:  $10 \text{ }\mu\text{m}$ ) containing the nanoparticles were placed on an ITO plate, and the mass signal intensities at  $m/z$  197 were evaluated.

Fig. 1 shows mass signal intensities plotted against the volumes of the nanoparticles. Diameters of the nanospheres are also shown in the upper X-axis. The filled-circles indicates the signal intensities of the nanospheres. The larger nanospheres gave higher signal intensities. When the volumes reached to about  $4 \times 10^4 \text{ nm}^3$ , the signal intensities were almost saturated.

The mass signal intensities of gold nanostars are shown as the open stars. The nanostars showed somewhat higher signals than those of the corresponding nanospheres. The largest enhancement, about 25%, was exhibited by nanostars with corresponding volumes to 30 and 35-nm nanosphere. It was shown that the star-shape did contribute to efficient LDI of gold ions from the nanoparticles. The thin and sharp tips on the nanostars would contribute to efficient LDI, but the signal enhancements were not so remarkable.

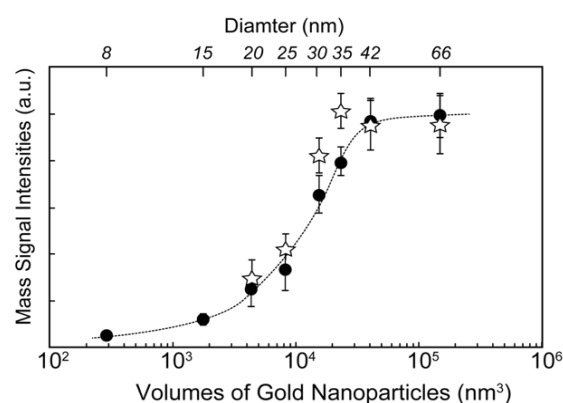


**Figure 2:** Mass signal intensities of gelatin sections containing nanosphere (filled-circle) and nanostars (open-stars).

#### References

1. T. Niidome, M. Fujii, N. Nakashima, Y. Katayama, and Y. Niidome, *Chem. Lett.* 44 (2015) 931.
2. M. Fujii, N. Nakashima, T. Niidome, and Y. Niidome, *Chem. Lett.* 43 (2014) 131.
3. D. Muko, T. Ikenaga, M. Kasai, J. B. Rabor, A. Nishitani, Y. Niidome, *J. Mass Spectrom.* 1 (2018) 54.
4. D. Muko and Y. Niidome, *Chem. Lett.* 47 (2018) 993.
5. D. Muko, Y. Inoue, A. Nishitani, and Y. Niidome, *Anal. Methods* 9 (2017) 1177.
6. Y. Inoue, O. Niihara, J. B. Rabor, T. Ikenaga, M. Kasai, Y. Niidome, *Chem. Lett.*, in press.

**5th IKCC, 9th November 2019**

**OIST Seaside House, Okinawa**

**POSTER CONTRIBUTIONS**

P01

## Morphological and Mechanical Characterization of Synthetic ECM to Suppress Cancer Metastasis

Sona Roy<sup>1</sup>, Sachie Yukawa<sup>1</sup>, William Cortes<sup>1</sup>, Ryo Kanno<sup>2</sup> and Ye Zhang<sup>1</sup>

1 Graduate School of Science and Technology, Okinawa Institute of Science and Technology

Imaging Research Section, Okinawa Institute of Science and Technology

2 Imaging Research Section, Okinawa Institute of Science and Technology

sachie.yukawa2@oist.jp

Metastasis, the ability of cancer cell to change position within the tissues through migration and invasion, represents the most deadly aspect of cancer. Cancer therapeutics that are designed to inhibit metastasis by targeting signaling pathways have not proven to be effective in clinical trials because cancer cells can modify their migration mechanism in response to different conditions. To cope with the dynamic transform, we developed a novel access to inhibit metastasis by tying up actin cytoskeleton through physical interaction to suppress cancer cell migration mechanically. We designed and synthesized self-assembly peptide chemically connected with integrin ligand. Binding with integrin, the peptides assembled into synthetic extracellular matrix (ECM) with nanoscale aspects on cancer cell membrane. The ECM chained together activated integrins to fixate and block their redistribution. The actin skeleton linked with integrins were tied up results into physically restrained cancer cell motility for metastasis inhibition.

P02



## Supramolecular amphiphilic systems based on resorcin[4]arene: self-assembly and drug-loading capacity

Ruslan Kashapov<sup>1</sup>, Yuliya Razuvayeva<sup>1,2</sup>, Albina Ziganshina<sup>1</sup>, Svetlana Lukashenko<sup>1</sup>, Anastasiya Sapunova<sup>1</sup>, and Lucia Zakharova<sup>1,2</sup>

<sup>1</sup> A.E. Arbuzov Institute of Organic and Physical Chemistry, Kazan Scientific Center, Russian Academy of Science, Kazan 420088, Russia

<sup>2</sup> Kazan National Research Technological University, Kazan 420015, Russia

kashapov@iopc.ru

The nanosized particles based on macrocyclic amphiphiles have been widely applied in biomedical applications such as drug delivery and targeting [1,2]. Their main advantages are nanoscale dimensions, low aggregation threshold, easy preparation and ability to encapsulate drug, the controlled release of which is an essential technique developed in order to increase the effectiveness and decrease the side effects in long-term administration of therapeutic agents. Here, we present synthesis of new resorcin[4]arene with N-methyl-D-glucamine groups on the upper rim and n-decyl chains on the lower rim, investigation of its self-assembly behavior in aqueous media, and its use as a building block for the formation of drug nanocontainer. N-methyl-D-glucamine fragments in the resorcin[4]arene structure promote a higher stability in solutions, simplification of self-aggregation and increased biological activity. Antimicrobial and hemolytic activity assessment revealed that this resorcin[4]arene obtained is non-toxic. The study of cell penetration was carried out with both free and encapsulated doxorubicin (DOX). Surprisingly, DOX-loaded macrocycle aggregates are more efficient in causing cell death and destroy the nucleus. Conceivably, this knowledge will help in the rational design of DOX combination for nucleus-target therapies.

This work was supported by Russian Science Foundation, grant no. 17-73-20253.

### References

- [1] W. Shao, X. Liu, T. Wang and X.-Y. Hu, *Chinese Journal of Organic Chemistry* **38** (2018) 1107.
- [2] J. Gao, J. Li, W.C. Geng, F.Y. Chen, X. Duan, Z. Zheng, D. Ding and D.S. Guo, *Journal of the American Chemical Society* **140** (2018) 4945.

Neha Sharma<sup>1,3</sup>, Mun'delANJI Vestergaard<sup>2</sup>, Shigeru Deguchi<sup>1</sup> and Masahiro Takagi<sup>3</sup>

1 Research Centre for Bioscience and Nanoscience,  
Japan Agency for Marine-Earth Science and Technology, Japan

2 Faculty of Agriculture, Kagoshima University, Japan

3 Bioscience and Biotechnology Area,  
Japan Advanced Institute of Science and Technology, Japan

[takagi@jaist.ac.jp](mailto:takagi@jaist.ac.jp)

Artificial lipid vesicles are a bioinspired technology that can be exploited to understand biological mechanisms. Our daily diet contains capsaicin, present in chilli and responsible for their hotness. Capsaicin shows analgesic [1], anti-cancer and inflammatory properties. Thus, to understand the mechanism behind its activity, we investigated the effect of capsaicin on binary and ternary lipid systems. We have shown that capsaicin promoted membrane fluctuation by increasing membrane excess area [2]. Membrane fluidity changed with the lipid composition. Capsaicin increased fluidity of 1,2-dioleoyl-sn-glycero-3-phosphocholine (DOPC) membranes, while it rigidified DOPC and cholesterol-based liposomes. In addition, capsaicin induced homogeneity by decreasing phase separation in ternary phase system (figure 1). We imagine this lipid re-organization to be associated with the physiological warming sensation upon consumption of capsaicin. Thus, the results will enhance understanding of biological properties of capsaicin.

#### References

[1] Caterina M.J. et al *Science* **288** (2000) 306.

[2] Sharma N. et al *Biomimetics* **4** (2019) 17.

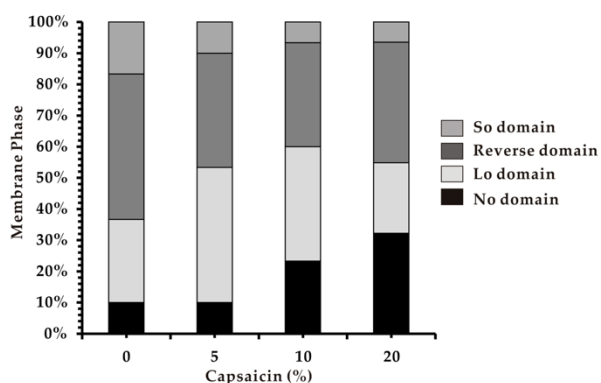


Figure 1. Phase-separation profile in DOPC/DPPC/Chol/Cap.

## Sedimentation Particle Size and Porosity Estimation by Differential Centrifugal Sedimentation

Yuichi Kato<sup>1</sup>, Takahiro Morimoto<sup>1</sup>, Kazufumi Kobashi<sup>1</sup>, Takeo Yamada<sup>1</sup>, Toshiya Okazaki<sup>1</sup>, and Kenji Hata<sup>1</sup>

<sup>1</sup> CNT-Application Research Center, National Institute of Advanced Industrial Science and Technology (AIST), Japan

toshi.okazaki@aist.go.jp

Measuring particle size distribution of dispersions in liquids is important for evaluating size reduction, dispersion stability, and film formation properties. Here we propose a method to estimate sedimentation particle size and porosity of sponge-like particles by differential centrifugal sedimentation.

We found a phenomenon that the Stokes diameter ( $D_{\text{stokes}}$ ) of carbon nanotube (CNT) aggregates decreases as the rotational velocity ( $\omega$ ) increases (Fig. 1) when it sediments in density gradient. This indicates that particle sedimentation can not be interpreted by the common Stokes equation (1),

$$u = \frac{\Delta\rho D_{\text{stokes}}^2 R \omega^2}{18\eta} \quad (1)$$

where  $u$  is the sedimentation velocity,  $\Delta\rho$  is the difference of density between particle (apparent particle density) and fluid,  $R$  is the disk radius, and  $\eta$  is the viscosity. The  $D_{\text{stokes}}$  is not suitable for representing particle size distribution for CNT aggregates. The Stokes diameter change can be explained by the buoyancy caused by the density difference between the inner fluid of the particle and the outer fluid (Fig. 1, inset illustration). This buoyancy slows the particle sedimentation. This difference in density depends on the sedimentation velocity  $u$ .

The corrected sedimentation particle diameter ( $D_{\text{corrected}}$ ) and porosity of the particle ( $\phi$ ) can be estimated based on the simple equation (2),

$$u = \frac{\Delta\rho(1-\phi)D_{\text{corrected}}^2 R \omega^2}{18\eta + \frac{\partial\rho_{f,o}}{\partial R} \phi D_{\text{corrected}}^4}{60D_d} R \omega^2 \quad (2)$$

where  $D_d$  is diffusion constant of sucrose,  $\frac{\partial\rho_{f,o}}{\partial R}$  is the density gradient.

### Reference

[1] Y. Kato, T. Morimoto, K. Kobashi, T. Yamada, T. Okazaki, K. Hata, The Journal of Physical Chemistry C **123** (2019) 21252-21256.

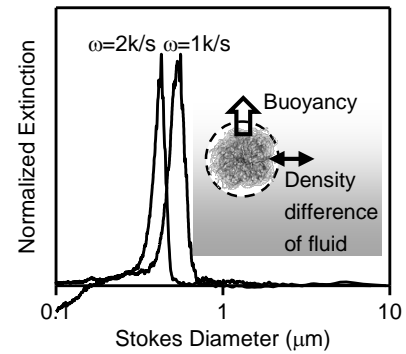


Fig. 1 Rotational speed dependent Stokes Diameter of CNT aggregates.



## Insights into the adsorption behavior of surfactant onto silica surface with polyelectrolytes

Zilong Liu<sup>1</sup>, Pegah Hedayati<sup>1</sup>, Ernst J. R. Sudhölter<sup>1</sup>, Robert Haaring<sup>1</sup>,  
Abdur Rahman Shaik<sup>1</sup>, and Naveen Kumar<sup>1</sup>

<sup>1</sup> Organic Materials & Interfaces, Department of Chemical Engineering, Delft University of Technology, The Netherlands

z.liu-6@tudelft.nl

Adsorption behavior of surfactants to reservoir rock surfaces is an important issue in oil recovery, especially in the process of alkaline surfactant flooding. However, the loss of surfactant by adsorption onto the rock surface makes surfactant economically unfeasible.<sup>1,2</sup> In this study, the adsorption behavior of an anionic alcohol alkoxy sulfate (AAS) surfactant onto silica was investigated with a Quartz Crystal Microbalance with Dissipation monitoring (QCM-D), allowing us for a real-time quantitative analysis of the adsorption process. The results demonstrated that adsorption of the surfactants slightly increased with increasing solution pH, suggesting that cation bridging played a significant role. The amount of adsorption varied as a function of the CaCl<sub>2</sub> concentration and did not increase from a certain concentration. In mixed cation solutions, it was confirmed that the Ca<sup>2+</sup> enhanced the adsorption of AAS, but Na<sup>+</sup> repressed the adsorption by competing for the binding sites. Adsorption isotherm of AAS was well described by the Langmuir model, while the adsorption behavior of a polyelectrolyte of polystyrene sulfonate (PSS) was best fitted with the Freundlich model. Co-injection experiments of an AAS+PSS mixture showed competitive adsorption behavior that the adsorbed amount of AAS was greatly reduced by the addition of PSS. These results contribute to a better understanding of the adsorption behavior of surfactant to silica surfaces and offer important clues for reducing surfactant loss by introducing polyelectrolyte sacrificial agents.

### References

- 1 M. Lashkarbolooki, S. Ayatollahi and M. Riazi, Mechanical study of effect of ions in smart water injection into carbonate oil reservoir, *Process Saf. Environ. Prot.*, 2017, **105**, 361–372.
- 2 S. Solairaj, C. Britton, D. H. Kim, U. Weerasooriya and G. A. Pope, in *SPE Improved Oil Recovery Symposium*, Society of Petroleum Engineers, 2012.



Fig. 1 Schematic of surfactant adsorption on a silica surface.

## Intentionally Added Ionic Surfactants Induce Jones-Ray Effect at Air-Water Interface

Yuki Uematsu<sup>1,3</sup>, Kengo Chida<sup>2</sup>, and Hiroki Matsubara<sup>2</sup>

1. Laboratoire de Physique, Ecole Normale Supérieure, Paris, France

2. Department of Chemistry, Kyushu University, Fukuoka, Japan

3. Department of Physics, Kyushu University, Fukuoka, Japan

uematsu.yuki@phys.kyushu-u.ac.jp

The Jones-Ray effect is a characteristic minimum in the surface tension of aqueous electrolytes at milli-molar salt concentrations [1]. We experimentally demonstrated that intentionally added ionic surfactants induce the minimum at milli-molar salt concentration [2]. The one-dimensional Poisson-Boltzmann theory, including the effect of surfactant adsorption and salt depletion [3], excellently agrees with the obtained experimental data. All the parameters of the ion-specific surface energies used in the theory are consistent with previous experiments of the surface tension. These results strongly suggest that the Jones-Ray effect observed so far has been induced by inevitable contamination of the air-water interfaces.

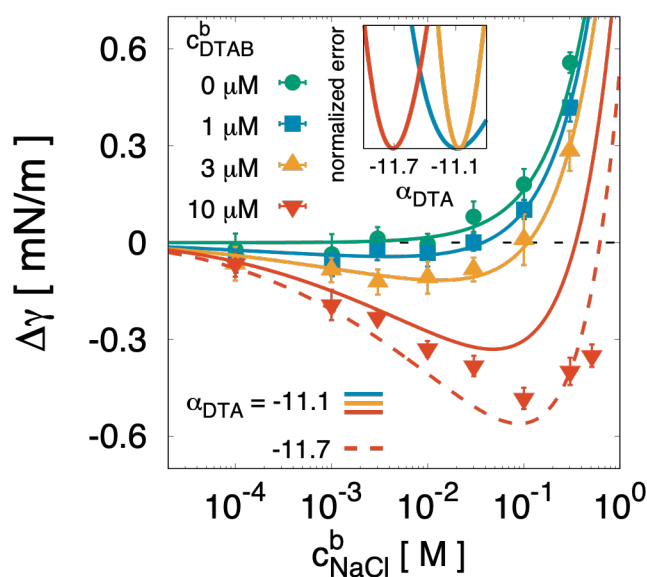


Fig. 1 Surface tension of the NaCl solutions in the absence and presence of DTAB surfactants. The points are the experimental data and the lines are the theoretical calculations. The inset shows the errors of the least-squares fits normalized by their minimum with varying the adsorption energy of DTA ion.

### References

- [1] G. Jones, and W.A. Ray, *J. Am. Chem. Soc.* **59**, 187–198 (1937).
- [2] Y. Uematsu, K. Chida, and H. Matsubara, *Coll. and Int. Sci. Comm.* **27**, 45-48 (2018).
- [3] Y. Uematsu, D. J. Bonhuis, and R. R. Netz, *J. Phys. Chem. Lett.* **9**, 189–193 (2018).

P07

## Aggregation behavior in cesium hydroxide-decanoic acid mixed solution

Taichi Koga, Masumi Villeneuve\*

Graduate school of Integrated Arts and Sciences, Hiroshima University

\*Graduate school of Integrated Sciences for Life, Hiroshima University

**Introduction:** Fatty acid soap solution has been studied over 100 years for both scientific and industrial interests. The complicated phase behavior of ternary system of fatty acid - alkali fatty acid - water is well known to be due to acid soap formation. Acid soap is a fixed stoichiometric ratio complex formed between the acid and the alkali soap owing to hydrogen bonding between the headgroups [1, 2]. However, the details of the aggregation behavior in dilute solutions are not clarified yet. In this study, dilute aqueous solution of mixture of cesium hydroxide (CsOH) and decanoic acid was investigated especially near the critical aggregate concentration (cac).

**Experiment:** Decanoic acid (assay:  $\geq 99.5\%$  GC, Fluka, Germany) was recrystallized from hexane, and from water/ethanol mixture. A CsOH (trace metal analysis:  $> 99.95\%$ , Sigma-Aldrich, Japan) aq. solution was titrated with an oxalic acid aq. solution to check its purity as a base before sample preparation. Surface tension  $\gamma$  was measured using the sessile bubble method. pH, dynamic light scattering (DLS), and small angle x-ray scattering (SAXS) were also measured. All the experiments were conducted at 298 K

**Results and Discussions:** A kink at  $m \approx 0.016 \text{ mmol kg}^{-1}$  on  $\gamma$  vs. concentration isotherm was ascribed as cac for the pure decanoic acid solution (Fig. 1). Cacs of all the mixed solutions were found at such low concentrations. According to thermodynamics, while up to two types of aggregate can coexist in a pure decanoic acid solution, at most three types of aggregate can coexist in a mixed CsOH-decanoic acid solution. In such situations, the surface tension will not depend on the total concentration. The DLS data of a pure decanoic acid in the concentration region where  $\gamma$  was kept constant yielded two distinct decay times, which was consistent with the thermodynamic prediction. Finally, the results of SAXS on a pure decanoic acid solution implied a structure having the interlamellar spacing of  $1.7 \text{ \AA}$ . Together with the DLS data, the aggregates were suggested to be multi-lamellar-vesicles.

### Reference

- [1] McBain, J. W. The Hydrolysis of Soap Solutions II. The Solubilities of Higher Fatty Acids. The Journal of The American Oil Chemist' Society, pages 40–41, February 1948.
- [2] Ekwall, P. and L Mandell. Solutions of alkali soaps and water in fatty acids. Kolloid-Zeitschrift und Zeitschrift für Polymere, 233(1-2):938–944, 1969.

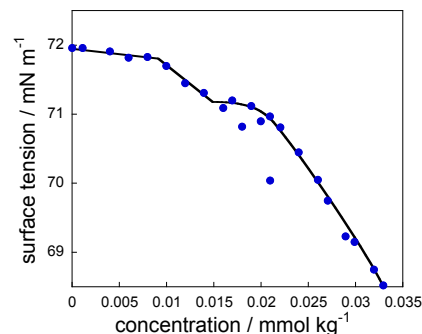


Figure 1. Surface tension vs. molality of pure decanoic acid solution at 298.15 K.

## Investigation of the adsorption of mixed nonionic surfactants at the liquid/solid interface by using QCM method

Sayuri Miyamoto<sup>1</sup>, Tomomi Nagasaka<sup>2</sup>, Kanna Hyodo<sup>2</sup>, and Norihiro Ikeda<sup>1,2</sup>

1 Graduate School of Health and Environmental Science.,  
Fukuoka Women's Univ, Japan

2 Faculty of Environmental Science, Fukuoka Women's Univ, Japan

[19mhe002@mb2.fwu.ac.jp](mailto:19mhe002@mb2.fwu.ac.jp)

### 1. Introduction

Various phase diagrams of adsorption of mixed surfactants at the vapor/liquid or liquid/liquid interface have been evaluated by analyzing the interfacial tension of the solution. On the other hands, there are few reports about the phase diagrams of adsorption at the liquid/solid interface due to being hard to measure the surface tension of solid. However, the phase diagram at the solid surface will give us important information about competitive adsorption or synergistic adsorption behavior on adsorbent. In this study, the adsorption of mixed nonionic surfactants (polyoxyethylene alkyl ether: CiEj) on the solid (gold electrode) surface from the solution was investigated by using QCM method. We proposed the method of evaluating phase diagrams of adsorption at liquid/solid interface.

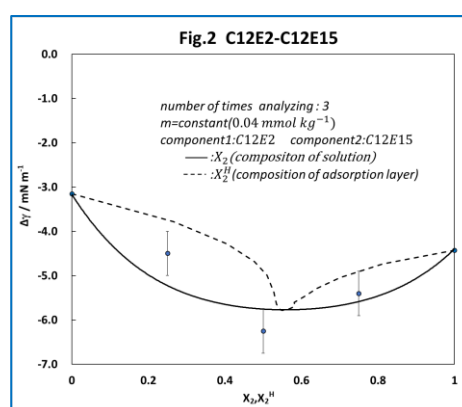
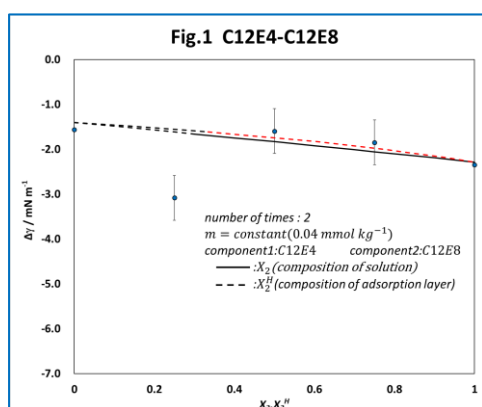
### 2. Experimental

The adsorption amounts at the solid surface were evaluated as a function of the total molality and composition of surfactants at 298.15 K by using QCM model NLQO-F21 (SUNRISE INDUSTRIAL CO.,LTD.) or QCM922A (SEIKO EG&G CO., LTD.). Moreover, surface tension of the aqueous solution was also measured by drop volume method to evaluate the corresponding phase diagram at the water/air interface.

### 3. Result and Consideration

Phase diagrams of adsorption at the CiEj mixture obtained at the gold surface are shown in Fig. 1 for C12E4-C12E8 system and in Fig. 2 for C12E2-C12E15 system. The C12E4-C12E8 mixture, in which the polyoxyethylene length differs only by two oxyethylene groups, shows a competitive adsorption of C12E8, whereas the C12E2-C12E5 mixture, in which the polyoxyethylene length largely differs, shows synergistic adsorption. This result suggests the phase diagrams can demonstrate characteristic behavior of adsorption at the solid surface.

In poster presentation, the result will be also compared with the corresponding phase diagram of liquid/vapor interface.



Keisuke Chiguchi<sup>1</sup>, Michael Gradzielski<sup>2</sup>, Law Bruce<sup>3</sup>, Hiroki Matsubara<sup>1</sup>

<sup>1</sup> Department of Chemistry, Faculty of Science, Kyushu University, Japan

<sup>2</sup> Institut für Chemie, Technische Universität Berlin, Germany

<sup>3</sup> Department of Physics, Kansas State University, USA

k.chiguchi@chem.kyushu-univ.jp

Particle-stabilized emulsion, so called Pickering emulsion offers enhanced stability over traditional surfactant stabilized emulsion. The physical properties of Pickering emulsion are closely related to the contact angle  $\theta$  of particles at liquid-liquid interface determined by the balance between the three interfacial tensions. However, for adsorbed nanoparticles, it is necessary to take into account of the contribution of line tension  $\tau$ . The line tension is an excess energy associated with the unit length of three phase contact and depending on the particle size.<sup>[1,2]</sup> In this study, we observed the demulsification of Pickering emulsions near the critical solution point of binary liquid mixtures and considered the relationship between line tension, contact angle and emulsion properties.

The water/2,6-lutidine mixture which has a lower critical solution temperature  $T_c$  was adopted as solvent and different sized hydrophilic silica particles (diameter : 10, 50, 100, 500 and 1000 nm) were used as emulsifier. When the Pickering emulsions were cooled from a high temperature to  $T_c$  at the critical weight fraction, the demulsification occurred at temperatures higher than  $T_c$  depending on the particle size (Fig.1). Emulsions prepared with smaller particles were more stable in wider temperature ranges, i.e., the demulsification temperature approached  $T_c$ . Considering these results based on the modified Young equation,  $\gamma_{PO} + \tau/r = \gamma_{PW} + \gamma_{OW} \cos\theta$ , a negative line tension was expected for the present system. We also calculated the particle size dependence of contact angle at given temperatures based on the estimated line tension values (Fig.2). As the particle size decreases, the contact angle increases and finally reaches  $90^\circ$  to maximize the contact line. The influence of contact angle on emulsion droplet size and stability were also discussed.

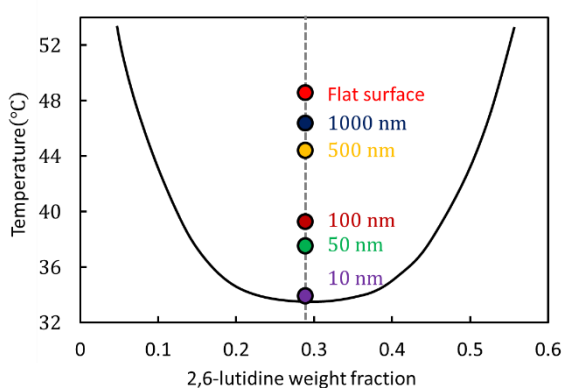


Fig.1 Demulsification temperature for different sized silica particles

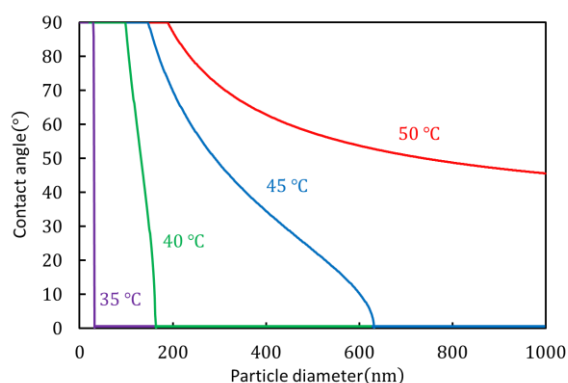


Fig.2 Particle size dependence of contact angle at water-lutidine interface

#### References

- [1] P. McBride and B. Law, *Physical Review Letters* 109, **2012**, 196101  
 [2] H. Matsubara, J. Otsuka and B. Law, *Langmuir* **2018**, 34, 331-340

## Effect of alcohols and cosmetic oils on O/W emulsions stabilized by surface freezing transition

H. Sakamoto<sup>1</sup>, Albert Praues<sup>2</sup>, Michael Gradzielski<sup>2</sup>, Hiroki Matsubara<sup>1</sup>

<sup>1</sup> Department of Chemistry, Faculty of Science, Kyushu University, Japan

<sup>2</sup> Institut für Chemie, Technische Universität Berlin, Germany

h.sakamoto@chem.kyushu-univ.jp

The penetration of alkane molecules into the adsorbed film gives rise to a surface freezing transition of cationic surfactant at the alkane-water interface upon cooling. In our previous study [1], it was demonstrated that the stability of oil-in-water (O/W) emulsions was greatly improved by the surface freezing transition of hexadecyltrimethylammonium chloride (HTAC) and tetradecane (C14) mixed adsorbed films. In this study, we performed similar experiments for the systems containing a long-chain alcohol, hexadecanol (C16OH), and a cosmetic oil, isopropyl parmitate (IPP).

Fig.1 shows the interfacial tension and ellipticity measured at the interface of HTAC aq. and dodecane solution of C16OH. The interfacial tension had a breakpoint at 23°C corresponding to the phase transition between surface liquid and frozen states and, at the same temperature, a rapid decrease in the ellipticity was observed. The stability of the O/W emulsion in the surface liquid and frozen states was compared in Fig.2. As observed in the previous study, the emulsion in the surface frozen state was more stable than that in the surface liquid state. However, the kinetic stability of the O/W emulsions was decreased compared with the HTAC-C14 system. Similar results were obtained also for the interface of HTAC aq. and the mixed solution of IPP and hexadecane (9:1 molar ratio). However, the phase transition temperature has a minimum against HTAC molality. We expected that the surface frozen film is composed of IPP and hexadecane below the minimum and is composed of HTAC and hexadecane above the minimum.

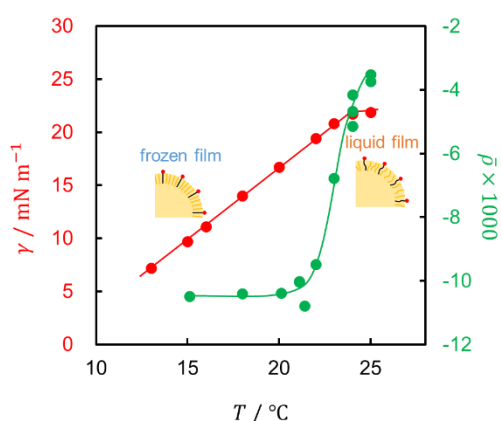


**Fig.1** Interfacial tension and ellipticity curve for the HTAC-C16OH system (concentration of HTAC in aqueous phase was  $0.4 \text{ mmol kg}^{-1}$  and that of C16OH in dodecane was  $10 \text{ mmol kg}^{-1}$ ).

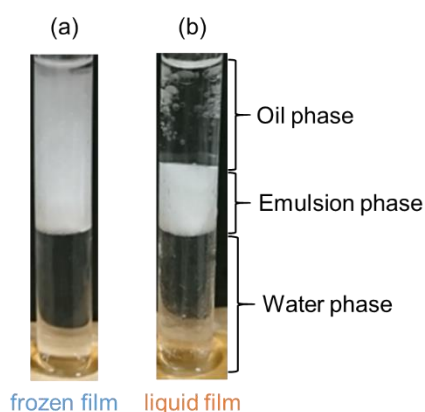


**Fig.2** Emulsion samples prepared with (a) surface frozen and (b) surface liquid films.

### References

[1] Y. Tokiwa, H. Sakamoto, T. Takiue, M. Aratono, H. Matsubara, *Effect of Surface Freezing on Stability of Oil-in-Water Emulsions*, 34(21) **2018**, 6205-6209.

## Control of line tension and fluid domain morphology by addition of hybrid phospholipid in ternary lipid vesicle

Ryoa Kanda<sup>1</sup>, Yosuke Imai<sup>2</sup>, and Takanori Takiue<sup>1,2</sup>

<sup>1</sup> Graduate School of Science, Kyushu University, Japan

<sup>2</sup> Faculty of Arts and Science, Kyushu University, Japan

r.kanda@chem.kyushu-univ.jp

Biological membrane is considered to express many membrane functions by forming in-plane minute heterogeneous structure called raft. In order to elucidate the complex behavior of biological membrane, lipid vesicles composed of phospholipid and cholesterol are often studied as its simplest model. These vesicles are known to phase-separate into liquid-ordered (Lo) and liquid-disordered (Ld) phases depending on the composition and temperature. Line tension is an excess energy at domain boundary and shorten the total length of the boundary line. Therefore, controlling line tension is crucial to manipulate domain morphology, which enables us to mimic valuable functions of biomembrane.

In this study, we adopted 3-component mixture: 1,2-dipalmitoyl-*sn*-glycero-3-phosphocholine (DPPC) / 1,2-dioleoyl-*sn*-glycero-3-phosphocholine (DOPC) / cholesterol (Chol). The effect of hybrid phospholipid (1-palmitoyl-2-oleoyl-*sn*-glycero-3-phosphocholine: POPC) on this system was investigated by quantifying line tension (flicker spectroscopy method) as function of POPC mole fraction coupled with change in domain morphology by fluorescence microscope at atmospheric pressure.

In DPPC/DOPC/Chol system, phase separation into Lo phase enriched in DPPC and Chol, and Ld one in DOPC was observed, as shown respectively by the dark and the bright regions in Fig.2. For the composition relatively far from the critical point in Lo/Ld coexistence in the ternary system without POPC, line tension of 0.6 - 1.0 pN (Fig.1) was obtained. As the molar fraction of POPC was increased with fixed molar ratio of DPPC/DOPC/Chol, line tension decreases gradually and the corresponding dispersed domain shape changes from circular in high to mosaic in low line tension region (roughly < 0.3 pN), and finally disappeared within a resolution of microscope. This result is attributed to the affinity of POPC for both DPPC and DOPC, that makes the physical properties of Lo and Ld phases similar.

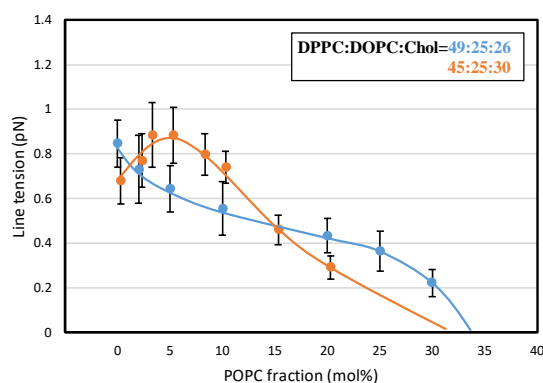


Fig.1 Line tension vs. POPC mole fraction

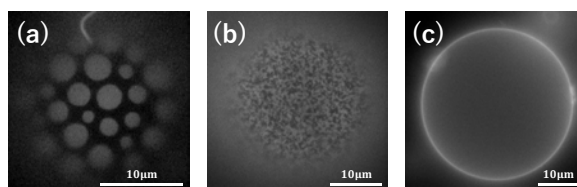


Fig.2 Domain morphology at each POPC mole fraction of (a) 5 mol%, (b) 30 mol%, (c) 35 mol%. The molar ratio of three components was fixed at DPPC:DOPC:Chol = 49:25:26.

## Molecular Miscibility and Domain formation in Mixed Adsorbed Film of Fluoroalkanols at Alkane/Water Interface

Runa Mitsuda<sup>1</sup>, Hajime Tanida<sup>2</sup>, Toshiaki Ina<sup>2</sup>, Kiyofumi Nitta<sup>2</sup>, Tomoya Uruga<sup>2</sup>, Yosuke Imai<sup>3</sup>, and Takanori Takiue<sup>1,3</sup>

<sup>1</sup> Graduate School of Science, Kyushu University, Japan

<sup>2</sup> Japan Synchrotron Radiation Research Institute, Japan

<sup>3</sup> Faculty of Arts and Science, Kyushu University, Japan

r.mitsuda@chem.kyushu-univ.jp

Adsorbed film at gas/liquid and liquid/liquid interfaces is generally regarded as a basic model of more complicated molecular organized systems such as biological membrane, emulsion and so on. In our previous study on the adsorbed film of hybrid alcohol, 2-perfluorooctylethanol ( $\text{CF}_3(\text{CF}_2)_7(\text{CH}_2)_2\text{OH}$ ; F8H2OH), it was shown that the adsorbed F8H2OH film at the hexane (C6)/water (W) interface takes three film states (gaseous, expanded and condensed state respectively) and is heterogeneous of the expanded state in which the condensed domains are surrounded by low density gaseous region.

In this study, we employed 6-perfluorohexylhexanol ( $\text{CF}_3(\text{CF}_2)_5(\text{CH}_2)_6\text{OH}$ ; F6H6OH) which consists of the same carbon number of fluorocarbon (FC) and hydrocarbon (HC) chains and thus is expected to show affinities with both F8H2OH and alkane molecules, and studied the effect of addition of F6H6OH on the state of the adsorbed F8H2OH films at alkane (C6 and C12)/W interfaces by interfacial tensiometry, X-ray reflectometry (XR), and Brewster angle microscopy (BAM).

The phase diagram of adsorption at C12/W interface (Fig.1), which gives a quantitative relation of the composition in bulk oil solution (solid line) and the adsorption film (dashed line) in equilibrium with each other, indicated that F8H2OH and F6H6OH are more miscible in the expanded film than in the condensed one. The electron density profile in the condensed state manifested that both components are densely packed with almost vertical orientation. XR data in the expanded state, on the other hand, suggested that the expanded film is heterogeneous structure in which condensed F8H2OH domains coexist with low density gaseous region and the domain coverage is larger at C6/W than at C12/W interface. BAM observation in the expanded film state at C6/W interface (Fig.2) clearly showed that as the film composition of F6H6OH increased, the domain size decreased and the coverage increased. This is mainly due to that F6H6OH molecules adsorb preferentially at the domain boundary and reduce domain line tension to promote the formation of many smaller domains.

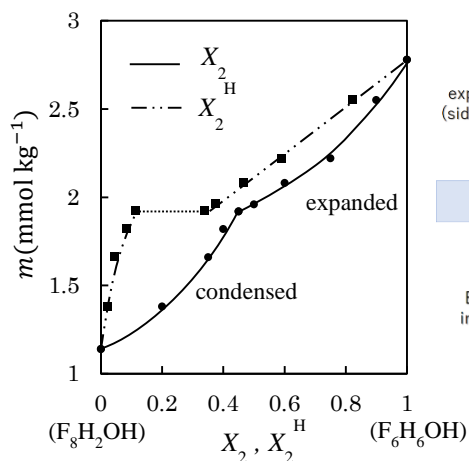


Fig.1. Phase diagram of adsorption at  $41 \text{ mN m}^{-1}$

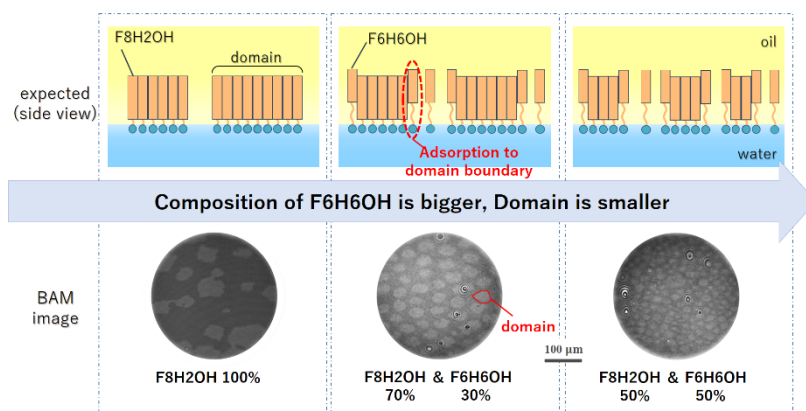


Fig.2. expected figure & BAM image at hexane/water

## Study on Effect of Hydrophilic Structure on Adsorption Behavior of Fluorinated Ester at Hexane/Water Interface

Tetsuya Hotta<sup>1</sup>, Toshiaki Ina<sup>2</sup>, Kiyofumi Nitta<sup>2</sup>, Tomoya Uruga<sup>2</sup>, Hajime Tanida<sup>3</sup>, Yosuke Imai<sup>4</sup>, and Takanori Takiue<sup>1,4</sup>

<sup>1</sup> Graduate School of Science, Kyushu University, Japan

<sup>2</sup> Japan Synchrotron Radiation Research Institute, Hyogo, 679-5198, Japan

<sup>3</sup> Sector of Nuclear Science Research, Japan Atomic Energy Agency, Japan

<sup>4</sup> Faculty of Arts and Science, Kyushu University, Japan

t.hotta@chem.kyushu-univ.jp

The adsorbed films at soft interfaces including liquid/liquid interface are regarded as fundamental model for more complicated self-organized systems, especially, in purpose of clarifying 2D heterogeneity such as “raft” in natural membranes. Among others, in our previous study, it was found that an expanded film of 2-perfluorooctyl-1-ethanol ( $F_8H_2OH$ ) at hexane/water interface is a heterogeneous structure in which condensed domains with several tens of  $\mu m$  coexist with low density gaseous region. Furthermore, the domain size becomes smaller by mixing of 6-perfluorohexyl-1-hexanol ( $F_6H_6OH$ ) at the interface due to reduction of “contact energy”, which is one of the contributions to “line tension” acting at domain boundary.<sup>[1,2]</sup> In this study, in order to discuss the effect of hydrophilic structure on the adsorbed film in relation to domain formation from the viewpoint of line tension, the adsorption of Methyl Perfluorolaurate (Me-PFLA) at hexane solution/water interface was examined by interfacial tensiometry, X-ray Reflectometry (XR), and Brewster Angle Microscopy (BAM).

The interfacial tension  $\gamma$  of Me-PFLA system was measured as a function of molality  $m_1$  and temperature  $T$  under atmospheric pressure. XR was performed at BL37XU in SPring-8 to determine the electron density profile normal to the interface and BAM was used to visualize domain morphology.

The  $\gamma$  value at low  $m_1$  increased monotonically with increasing  $T$ , whereas, at high  $m_1$ , each  $\gamma$  vs.  $T$  curve has one break point due to the phase transition of the adsorbed film. The interfacial density  $\Gamma^H$  increased with increasing  $m_1$ , changed discontinuously at the phase transition point, and then reaches a saturated value assuming that Me-PFLA molecules were closely packed at the interface ( $5.8 \mu mol m^{-2}$ ). Thus, it is plausible that the adsorbed film shows a gaseous (or expanded)-condensed phase transition at the interface. The electron density profile of the condensed film demonstrated that Me-PFLA molecules take a staggered arrangement to reduce steric and dipole-dipole repulsion between neighboring methyl ester groups (*Fig. 1*). The effect of hydrophilic structure on domain morphology will be discussed in terms of line tension on the basis of competitive model by McConnell.

[2]

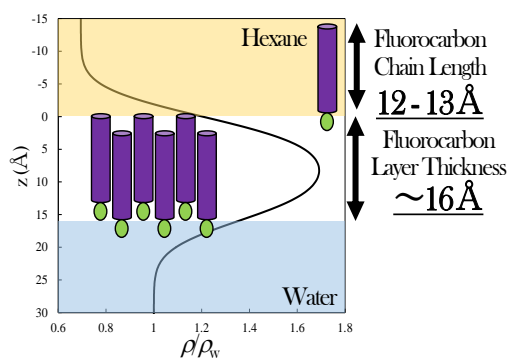


**Fig. 1.** Electron density profile and Schematic of condensed film

[1] K. Mitani *et al.*, *J. Phys. Chem. B* **119** (2015) 38

[2] H. McConnell, V. Moy, *J. Phys. Chem.* **92** (1998) 15

## Domain Formation and Molecular Miscibility in the Adsorbed Films of Mixed Fluoroalkanol-Cationic Surfactant System at Hexane/Water Interface

Chikara Shirai<sup>1</sup>, Kosuke Saiki<sup>1</sup>, Toshiaki Ina<sup>3</sup>,  
Kiyofumi Nitta<sup>3</sup>, Tomoya Uruga<sup>3</sup>, Hajime Tanida<sup>4</sup>,  
Yosuke Imai<sup>2</sup>, and Takanori Takiue<sup>1,2</sup>

1 Graduate School of Science, Kyushu University, Japan

2 Faculty of Arts and Science, Kyushu University, Japan

3 Japan Synchrotron Radiation Research Institute, Hyogo, 679-5198, Japan

4 Sector of Nuclear Science Research, Japan Atomic Energy Agency

whitepower@chem.kyushu-univ.jp

In this study, The effect of added cationic surfactant on the morphology of the domain formed by fluorocarbon alcohol was examined in the adsorbed films of H<sub>8</sub>H<sub>2</sub>OH (perfluorooctyl-2-ethanol) and dodecyltrimethylammonium bromide (DTAB) mixture by interfacial tension measurement and X-ray reflectometry. In addition, using BAM (Brewster angle microscope), I was observing the shape of the domain. Experiments were carried out on the mixed adsorbed film at the interface between F<sub>8</sub>H<sub>2</sub>OH hexane solution of molality  $m_1^0$  and DTAB aqueous solution of molality  $m_2^W$ .

Fig.1 shows the phase diagram of adsorption showing the relationship between the composition in the bulk solution and that in the adsorbed film[1]. Condensed state (C) and two expanded states (E<sub>1</sub>, E<sub>2</sub>) were confirmed. For E<sub>2</sub>-C phase transition, hetero-azeotrope was observed, indicating that the weak interactions between fluorocarbon and hydrocarbon chains leads to immiscibility of F<sub>8</sub>H<sub>2</sub>OH and DTAB[2]. On the other hand in the C state, DTAB and F<sub>8</sub>H<sub>2</sub>OH were clearly mixed and the negative azeotrope was observed. This means that hydrophilic parts cause the stronger interaction between different molecules than that between the same ones. From BAM observation, condensed film domain formation was confirmed around E<sub>2</sub>-C transition point as shown in Fig.2. By adding DTAB to the single F<sub>8</sub>H<sub>2</sub>OH system, the domain morphology changed to rounded shape from square one and the size was increased. By further increasing of the proportion of DTAB, the domain size was reduced although the shape of the domain did not change. It is presumed that the contact energy became dominant in the first change, and has the dipole-dipole repulsion between neighboring molecules become dominant in the second change [3]. In the presentation, the results of x-ray reflectance measurement will be shown to discuss the domain formation from the viewpoint of electron density profile and domain coverage.

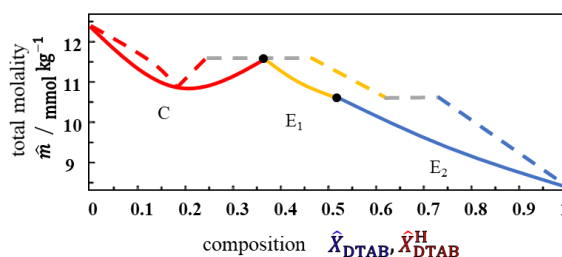
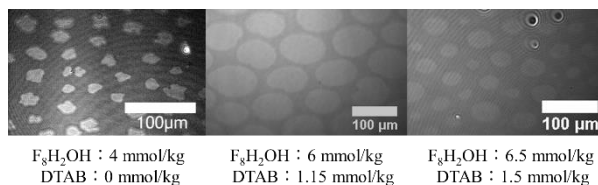


Figure 1. This phase diagram shows the relationship between the composition of the bulk solution and the adsorbed film at  $\gamma=25$  in equilibrium. Solid line composition of the bulk solution, the dotted line represents the composition of the adsorbed film. The red lines are condensed film, yellow lines and blue lines are expansion membranes E1 and E2. The gray dotted lines represents the phase transition of the adsorbed film and changes discontinuously.



### References

- [1] M. Aratono, M. Villeneuve, T. Takiue, N. Ikeda, H. Iyota, *J. Colloid Interface Sci.* 1998, 200, 161.
- [2] Takanori Takiue et al, *J. Phys. Chem. B* 1998, 102, 5840.
- [3] H. M. McConnell, V. T. Moy, *J. Phys. Chem.* 1988, 92, 4520.